

AD

TECHNICAL REPORT ARBRL-TR-02394

TWO AND THREE-DIMENSIONAL OBLIQUE  
IMPACT COMPUTATIONS

V. Kucher

February 1982



US ARMY ARMAMENT RESEARCH AND DEVELOPMENT COMMAND  
BALLISTIC RESEARCH LABORATORY  
ABERDEEN PROVING GROUND, MARYLAND

Approved for public release; distribution unlimited.

Destroy this report when it is no longer needed.  
Do not return it to the originator.

Secondary distribution of this report by originating  
or sponsoring activity is prohibited.

Additional copies of this report may be obtained  
from the National Technical Information Service,  
U.S. Department of Commerce, Springfield, Virginia  
22161.

The findings in this report are not to be construed as  
an official Department of the Army position, unless  
so designated by other authorized documents.

*The use of trade names or manufacturers' names in this report  
does not constitute endorsement of any commercial product.*

## UNCLASSIFIED

SECURITY CLASSIFICATION OF THIS PAGE (When Data Entered)

REPORT DOCUMENTATION PAGE		READ INSTRUCTIONS BEFORE COMPLETING FORM
1. REPORT NUMBER Technical Report ARBRL-TR-02394	2. GOVT ACCESSION NO.	3. RECIPIENT'S CATALOG NUMBER
4. TITLE (and Subtitle)  TWO AND THREE-DIMENSIONAL OBLIQUE IMPACT COMPUTATIONS		5. TYPE OF REPORT & PERIOD COVERED  FINAL
7. AUTHOR(s)  V. Kucher		6. PERFORMING ORG. REPORT NUMBER
9. PERFORMING ORGANIZATION NAME AND ADDRESS  US Army Ballistic Research Laboratory (ATTN: DRDAR-BLT) Aberdeen Proving Ground, MD 21005		10. PROGRAM ELEMENT, PROJECT, TASK AREA & WORK UNIT NUMBERS  1L161102AH43
11. CONTROLLING OFFICE NAME AND ADDRESS US Army Armament Research and Development Command US Army Ballistic Research Laboratory (ATTN: DRDAR-BL) Aberdeen Proving Ground, MD 21005		12. REPORT DATE February 1982
14. MONITORING AGENCY NAME & ADDRESS (if different from Controlling Office)		13. NUMBER OF PAGES 39
		15. SECURITY CLASS. (of this report)  UNCLASSIFIED
		15a. DECLASSIFICATION/DOWNGRADING SCHEDULE
16. DISTRIBUTION STATEMENT (of this Report)  Approved for public release; distribution unlimited.		
17. DISTRIBUTION STATEMENT (of the abstract entered in Block 20, if different from Report)		
18. SUPPLEMENTARY NOTES		
19. KEY WORDS (Continue on reverse side if necessary and identify by block number) Penetration mechanics Two-dimensional computer code Three-dimensional computer code Eulerian computer code Shaped-charge penetration		
20. ABSTRACT (Continue on reverse side if necessary and identify by block number)  The oblique impact of a shaped-charge jet is simulated by a plate-on-plate (plane strain) impact by the TRIDORF code operating in a two-dimensional, Cartesian mode. The effects of varying the thickness of the penetrator plate on penetration history, target hole size, pressure field history, and the bulge size on the back face of the target plate are examined. These impact phenomena were compared to the results obtained by running the TRIDORF code in a three-dimensional, Cartesian mode and simulating the shaped-charge jet impact by a bar impacting on a target plate.		

## TABLE OF CONTENTS

	Page
LIST OF ILLUSTRATIONS. . . . .	5
I. INTRODUCTION . . . . .	7
II. COMPUTER CODE. . . . .	8
III. THREE-DIMENSIONAL IMPACT . . . . .	8
IV. TWO-DIMENSIONAL IMPACTS. . . . .	10
V. DISCUSSION . . . . .	11
VI. CONCLUSIONS. . . . .	13
REFERENCE LIST . . . . .	35
DISTRIBUTION LIST. . . . .	37

**This page Left Intentionally Blank**

## LIST OF ILLUSTRATIONS

Figure	Page
1. Penetrator-Target Geometries. . . . .	14
2. Three-Dimensional Coordinate System . . . . .	15
3. Penetrator-Target Configuration in the Plane of Symmetry. . . . .	16
4. Penetrator-Target Deformation at 0 $\mu$ s . . . . .	17
5. Penetrator-Target Deformation at 5 $\mu$ s . . . . .	18
6. Penetrator-Target Deformation at 10 $\mu$ s. . . . .	19
7. Penetrator-Target Deformation at 15 $\mu$ s. . . . .	20
8. Penetrator-Target Deformation at 20 $\mu$ s. . . . .	21
9. Penetrator-Target Deformation at 24 $\mu$ s. . . . .	22
10. Material Density Plots in the Plane of Symmetry at 1- $\mu$ s Intervals. . . . .	23
11. Material Density Plots in the Plane of Symmetry at 1- $\mu$ s Intervals. . . . .	25
12. Material Density Plots in Various Z-Planes at 10 $\mu$ s . . .	27
13. Material Density Plots in Various Z-Planes at 20 $\mu$ s . . .	29
14. Comparison of Pressure Fields at 2 $\mu$ s . . . . .	31
15. Comparison of Pressure Fields at 10 $\mu$ s. . . . .	32
16. Comparison of Pressure Fields at 15 $\mu$ s. . . . .	33
17. Comparison of Pressure Fields at 20 $\mu$ s. . . . .	34

**This page Left Intentionally Blank**

## I. INTRODUCTION

For several years hypervelocity, normal impact problems have been solved at the Ballistic Research Laboratory by two-dimensional, cylindrically symmetric, Eulerian, hydrodynamic computer codes with strength options.<sup>1</sup> The penetration of a target by a continuous shaped-charge jet<sup>2</sup> is an example of the type of problem suited for these codes and this is the problem that is addressed in this report. Since more and more impact problems of interest are asymmetric in nature (such as oblique impacts) and computers have become larger in memory capacity and faster in operation, three-dimensional, Eulerian, hydrodynamic computer codes with elastic-plastic features have been pressed into service over the past few years. Compared to two-dimensional codes, these three-dimensional codes, for comparable computational grids, require more computational cells and, therefore, longer running times.

If the cost of running a three-dimensional code is prohibitive, or, if a three-dimensional code is not available, a two-dimensional (plane strain) simulation of a three-dimensional impact problem is utilized. The validity of these two-dimensional computations was examined for normal impacts insofar as shock wave propagation, penetration history, crater size, and spallation were affected.<sup>3</sup> In this study, the validity of plane strain computations of a continuous shaped-charge jet obliquely impacting a target is examined.

The problem to be studied is the penetration and perforation of a 12.7-mm steel plate by a continuous, copper, shaped-charge jet at an obliquity of 77.5°. The jet is simulated by an 8-mm-diameter, semi-infinite, copper rod having a uniform velocity of 8.1 km/s prior to impact.

Three-dimensional, Eulerian codes are normally written in the Cartesian (x, y, z) coordinate mode. Because of the small diameter of the shaped-charge rod in relation to the other dimensions in the problem, the circular cross section of the rod is approximated by a square cross section of equal area. A pictorial view of a shaped-charge bar impacting a target at an angle is shown in Figure 1. When the code is utilized in the two-dimensional (plane strain) mode, the problem appears in a slab geometry as shown in Figure 1.

---

<sup>1</sup>John T. Harrison, "The History of the Utilization of Eulerian Hydrodynamic Computer Codes at the Ballistic Research Laboratory," *Transactions of the Twenty-Fifth Conference of Army Mathematics*, ARO Report 80-1, Jun 1979.

<sup>2</sup>V. Kucher and J. Harrison, "Shaped-Charge Jet Penetration of Discontinuous Media," *Ballistic Research Laboratory Report No. 1995*, Jul 1977.  
(AD #A043845)

<sup>3</sup>V. Kucher, "One, Two, and Three-Dimensional Impact Computations," *Ballistic Research Laboratory Report ARBRL-TR-02099*, Aug 1979.  
(AD #A060611)

## II. COMPUTER CODE

The TRIDORF code<sup>4</sup> was used to generate data for the two and three-dimensional treatments of the obliquity impact problem. TRIDORF is a three-dimensional, multimaterial, continuous, Eulerian, hydrodynamic code with an elastic-plastic strength option. Also as an option, the code employs tracer particles which play a passive role in the computations and are valuable in providing a "Lagrangian look" to the plotted output of the penetrator-target deformation. Tillotson's form<sup>5</sup> of the equation of state is incorporated into the code. The TRIDORF code was run on the CDC 7600 at the Ballistic Research Laboratory/ARRADCOM.

## III. THREE-DIMENSIONAL IMPACT

The TRIDORF code was used to solve the following problem: The penetration and perforation of an infinite steel plate, 12.7-mm thick, impacted upon by a semi-infinite, copper bar at 8.1 km/s and at an obliquity of 77.5°. The cross section of the bar was a 7.0898-mm square, approximating the cross-sectional area of a 8-mm-diameter rod.

The coordinate system used in the TRIDORF code is shown in Figure 2. From the geometry of the problem, the z-coordinate plane was selected as the plane of symmetry. The penetrator-target configuration in this plane is shown in Figure 3. Table I gives the grid coordinates and cell dimensions: dx, dy, and dz. The indices of the cells are I, J, and K in the x, y, and z directions, respectively.

The overall size of the grid was 120 mm by 310 mm by 50 mm with a corresponding grid size of 36 by 52 by 17 computational cells in the x, y, and z-directions, respectively. The non-uniform grid that was used resulted in a rectangular prism as a computational cell.

The z-coordinate plane, the plane of symmetry, was given the reflective boundary condition option. All the other planes bounding the computational grid were given transmittive boundary conditions in order to simulate an infinite target plate and to permit the flow of material out of the computational region. Since the bar's initial motion was in the positive y-direction, the boundary condition for that part of the y-coordinate plane near the bar was specified to feed bar material into the grid as a simulation of a semi-infinite bar.

The cells, occupying the initial volume of the copper penetrator, were given the following initial conditions:

<sup>4</sup>W. E. Johnson, "TRIDORF - A Two-Material Version of the TRIOIL Code with Strength," Computer Code Consultants, CCC-976, Sep 1976.

<sup>5</sup>J. H. Tillotson, "Metallic Equations of State for Hypervelocity Impact," Gulf General Atomic, GA-3216, Jul 1962.

Table I. Grid Coordinates and Cell Dimensions

<u>I</u>	<u>x (mm)</u>	<u>dx (mm)</u>	<u>J</u>	<u>y (mm)</u>	<u>dy (mm)</u>	<u>K</u>	<u>z (mm)</u>	<u>dz (mm)</u>
1	8.19555	8.19555	1	127.71	127.71	1	1.77245	1.77245
2	6.32190	14.51745	2	2.94	150.65	2	1.77245	5.54490
3	5.49730	20.01475	3	2.35	133.00	3	1.77245	5.31735
4	4.78020	24.79495	4	2.15	135.15	4	1.77245	7.08980
5	4.15670	28.95165	5	2.15	137.30	5	1.77245	8.86225
6	3.61450	32.56615	6	2.15	139.45	6	1.77245	10.63470
7	3.14310	35.70925	7	2.15	141.60	7	1.77245	12.40715
8	2.73310	38.44235	8	2.15	143.75	8	1.79710	14.20425
9	2.37660	40.81895	9	2.15	145.90	9	2.06660	16.27085
10	2.06660	42.88555	10	2.15	148.05	10	2.37660	18.64745
11	1.79710	44.68265	11	2.25	150.30	11	2.73310	21.38055
12	1.77245	46.45510	12	2.30	152.60	12	3.14310	24.52365
13	1.77245	48.22755	13	2.40	155.00	13	3.61450	28.13815
14	1.77245	50.00000	14	2.50	157.50	14	4.15670	32.29485
15	1.77245	51.77245	15	2.60	160.10	15	4.78020	37.07505
16	1.77245	53.54490	16	2.70	162.80	16	5.49730	42.57235
17	1.77245	55.31735	17	2.80	165.60	17	7.42765	50.00000
18	1.77245	57.08980	18	2.90	168.50			
19	1.77245	58.86225	19	2.90	171.40			
20	1.77245	60.63470	20	2.90	174.30			
21	1.77245	62.40715	21	2.90	177.20			
22	1.77245	64.17960	22	2.90	180.10			
23	1.77245	65.95205	23	2.90	183.00			
24	1.77245	67.72450	24	2.90	185.90			
25	1.77245	69.49695	25	2.90	188.80			
26	1.79710	71.29405	26	2.90	191.70			
27	2.06660	73.36065	27	2.90	194.60			
28	2.37660	75.73725	28	2.90	197.50			
29	2.73310	78.47035	29	2.90	200.40			
30	3.14310	81.61345	30	2.90	203.30			
31	3.61450	85.22795	31	2.90	206.20			
32	4.15670	89.38465	32	2.90	209.10			
33	4.78020	94.16485	33	2.90	212.00			
34	5.49730	99.66215	34	2.90	214.90			
35	6.32190	105.98405	35	2.90	217.80			
36	14.01595	120.00000	36	2.90	220.70			
			37	2.90	223.60			
			38	2.90	226.50			
			39	2.90	229.40			
			40	2.90	232.30			
			41	2.90	235.20			
			42	2.90	238.10			
			43	2.90	241.00			
			44	2.90	243.90			
			45	2.90	246.80			
			46	3.00	249.80			
			47	4.00	253.80			
			48	5.00	258.80			
			49	6.00	264.80			
			50	7.00	271.80			
			51	8.00	279.80			
			52	30.20	310.00			

1. Density = 8.9 Mg/m<sup>3</sup>
2. Pressure = 0.0 Mbar
3. x-component of velocity = 0.0 km/s.
4. y-component of velocity = 8.1 km/s.
5. z-component of velocity = 0.0 km/s.
6. Specific internal energy = 0.0 J/g.

Similar initial conditions were given to the cells occupying the initial volume of the target except that the density was that of the steel target material, 7.86 Mg/m<sup>3</sup>, and the y-component of the velocity was zero.

#### IV. TWO-DIMENSIONAL IMPACTS

The TRIDORF code, in the two-dimensional mode, was used to solve the following problems: The penetration and perforation of a steel plate, 12.7-mm thick, impacted upon by a copper plate at 8.1 km/s at an obliquity of 77.5°. Two thicknesses were considered for the copper plate: 3 mm and 5 mm.

The two-dimensional grid was similar to the grid that was used in the z-coordinate plane in the three-dimensional impact problem except that extra columns of cells were added along the length of the penetrators so that the penetrators would be 4 cells wide. This is the minimum number of cells for obtaining reasonable results.<sup>6</sup> The width of each of these four cells in the three-dimensional problems was 1.77245 mm. The width of each of these four cells in the two-dimensional impact problems was 0.75 mm and 1.25 mm for the 3-mm and 5-mm-wide penetrators, respectively. Since the minimum cell dimension plays a role in controlling the time increment for each cycle of computations, it was expected that the 3-mm impact problem would require more computational cycles than the three-dimensional problem and the two-dimensional, 5-mm-plate impact problem to reach the same time in the penetration process. Also the latter problem would require more computational cycles than the three-dimensional impact problem to reach this same time.

All the boundaries of the computational grid were given transmittive boundary conditions so that the infinite target plate could be simulated and the flow of material would be permitted out of the grid rather than reflected back. Since the penetrator plate's initial motion was in the positive y-direction, material was fed into this plate at the bottom boundary to simulate a semi-infinite plate.

The initial conditions in each cell of the grid were the same as those described for the three-dimensional impact problem except that, of course, the z-component of velocity was not included.

---

<sup>6</sup> V. Kucher, "Preliminary Computer Computations for Slender Rod Impact Problems," Ballistic Research Laboratory Report No. 1957, Feb 1977. (AD #A036995)

## V. DISCUSSION

In discussing the three impact problems, three identification codes will be used:

1. 3D-7 for the three-dimensional problem of a bar impacting on a target plate.
2. 2D-3 for the two-dimensional problem of a 3-mm plate impacting on a target plate.
3. 2D-5 for the two-dimensional problem of a 5-mm plate impacting on a target plate.

For comparison of the 3D-7 results with the 2D-3 and 2D-5 results, the 3D-7 results will be presented from the z-coordinate plane (the plane of symmetry).

The deformation of the penetrator-target configuration can be pictured by using tracer particles. Hundreds of these particles were positioned along the free surfaces of the penetrator and target. These positions were line-plotted in order to outline the penetrator and target materials. If two tracer particles which were initially relatively close to one another are, at a later time, separated by a relatively large distance, these particles will be connected graphically by a line which may seem to be plotted incorrectly. However, the end points of the line have been determined correctly.

In order to follow the positions of material which is internal to a penetrator or a target, tracer particles were positioned initially inside the free surfaces of the penetrator and target and symbol plotted to identify penetrator material and target material. Triangles were used to mark penetrator material, and squares, target material.

Figure 4 shows the tracer particle plots at the time of initial contact between the target and penetrator for 3D-7, 2D-3, and 2D-5. At 5  $\mu$ s (Figure 5) the back of the targets have a bulge, which indicates that the shock wave that was created due to the impact of the penetrator on the target has been reflected from the back surface of the target plate. The amplitude of the bulge is least for 3D-7 and the greatest for 2D-5. The lip on front side of the target away from the penetrator is smallest for 3D-7. These observations also hold true for later times (Figures 6 through 9). Notice the appearance of the long lines that connect tracer particles that were initially relatively close together.

Normal impact computations<sup>3</sup> also determined that the thinner penetrator plate more closely approximated the size of the bulge on the back surface of the target when compared to the cylindrically symmetric case of a rod impacting on a target.

Problem 3D-7 was also run by Wallace Johnson, Computer Code Consultants, Inc. under Contract No. DAAK11-77-0058, Department of the Army. Figures 10 and 11 show, at 1  $\mu$ s intervals of time, the material density plots from 1  $\mu$ s to 20  $\mu$ s in the plane of symmetry. The target material is coded blue; the penetrator material, red. These figures indicate that after 10  $\mu$ s, the density of the bulging material on the back of the target is of low density. Also the material being ejected from the front side of the target and from the penetrator appears to be of low density. These observations were not as vivid in the tracer particle plots (Figures 5 through 9).

In Figure 12, which was also supplied by Wallace Johnson, the time of penetration is fixed at 10  $\mu$ s at which time penetrator-target density plots are shown in planes that are parallel to the plane of symmetry. These plots are useful for constructing the crater size at this particular time. Again the target material is shown in blue; the penetrator material, in red. The red penetrator clearly appears in planes  $z = 0.9$  and  $2.7$  mm. In plane  $z = 4.4$  mm, the solid penetrator material does not appear because the half-thickness of the bar was 3.5449 mm. At plane  $z = 4.4$  mm through plane  $z = 9.7$  mm, some of the red penetrator material is evident, thus indicating penetrator flow in the third dimension,  $z$ . At plane  $z = 15.2$  mm, very little disturbance of the target material is evident.

Figure 13 is a density plot similar to Figure 12 except that the time of penetration is fixed at 20  $\mu$ s. The penetrator (red) has already perforated the target (blue). The hole in the target is clearly displayed in this series of pictures at various  $z$ -planes.

Further insight into the comparison of the three-dimensional problem with the two-dimensional problems is gained by analysis of the pressure fields. In 3D-7, the pressure field is plotted in the plane of symmetry. Upon examining Figures 14 through 17, it is evident that the peak pressure is the highest in 2D-5 and the lowest in 3D-7. This indicates that the four sides of the bar relieve the impact pressure more quickly than the two sides of the penetrator plates of 2D-3 and 2D-5. This accounts for the largest bulge of the back of the target occurring for 2D-5.

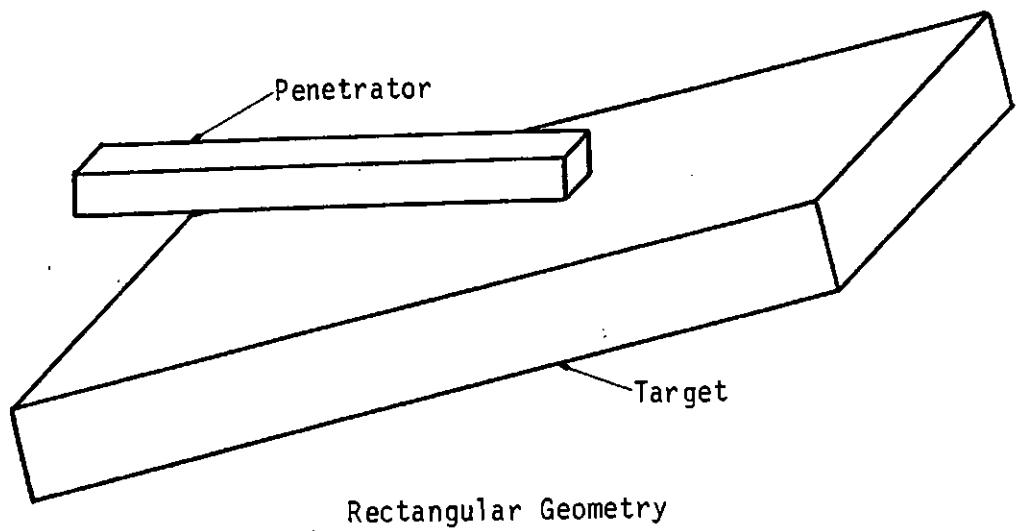
Normal impact computations<sup>3</sup> indicated that a thicker penetrator plate perforated a target sooner than a thinner penetrator plate; however, a penetrator bar or rod perforated the target the fastest. These results hold true for this oblique impact study as observed on the bulge on the back face of the target along the center line of the penetrators in Figure 8 at 20  $\mu$ s.

Figure 5 shows that neither of the slab impacts approximate the size of the lip being formed on the upper front face of the target or the direction of the ricochetting penetrator material. Of the two slab impacts, the 2D-5 case more closely approximates the 3D-7 direction of the ricochetting penetrator material.

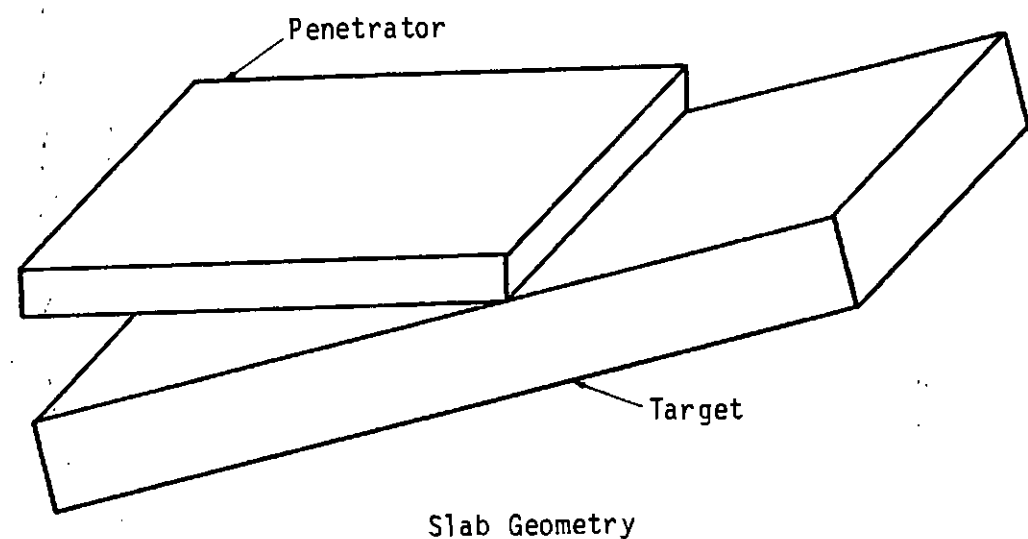
At 24  $\mu$ s (Figure 9) the widths of the holes in the targets for 3D-7 and 2D-5 are about the same; the hole for 2D-3 is smaller. This conforms with the results from normal impact computations<sup>3</sup> which showed that, by selecting the proper thickness for a penetrator slab, the hole or crater size computed by a three-dimensional code could be closely approximated.

## VI. CONCLUSIONS

Two-dimensional impact codes serve as a useful tool for approximating certain phenomena associated with oblique shaped-charge jet impact. These phenomena include penetration history, hole or crater size, pressure field history, and bulge size on the back face of a target. By adjusting the thickness of the penetrator slab, certain phenomena can be closely approximated; however, there does not seem to be one thickness that can closely approximate all of the phenomena that are observed from three-dimensional computations simulating the impact of a shaped-charge jet.



Rectangular Geometry



Slab Geometry

Figure 1. Penetrator-Target Geometries

15

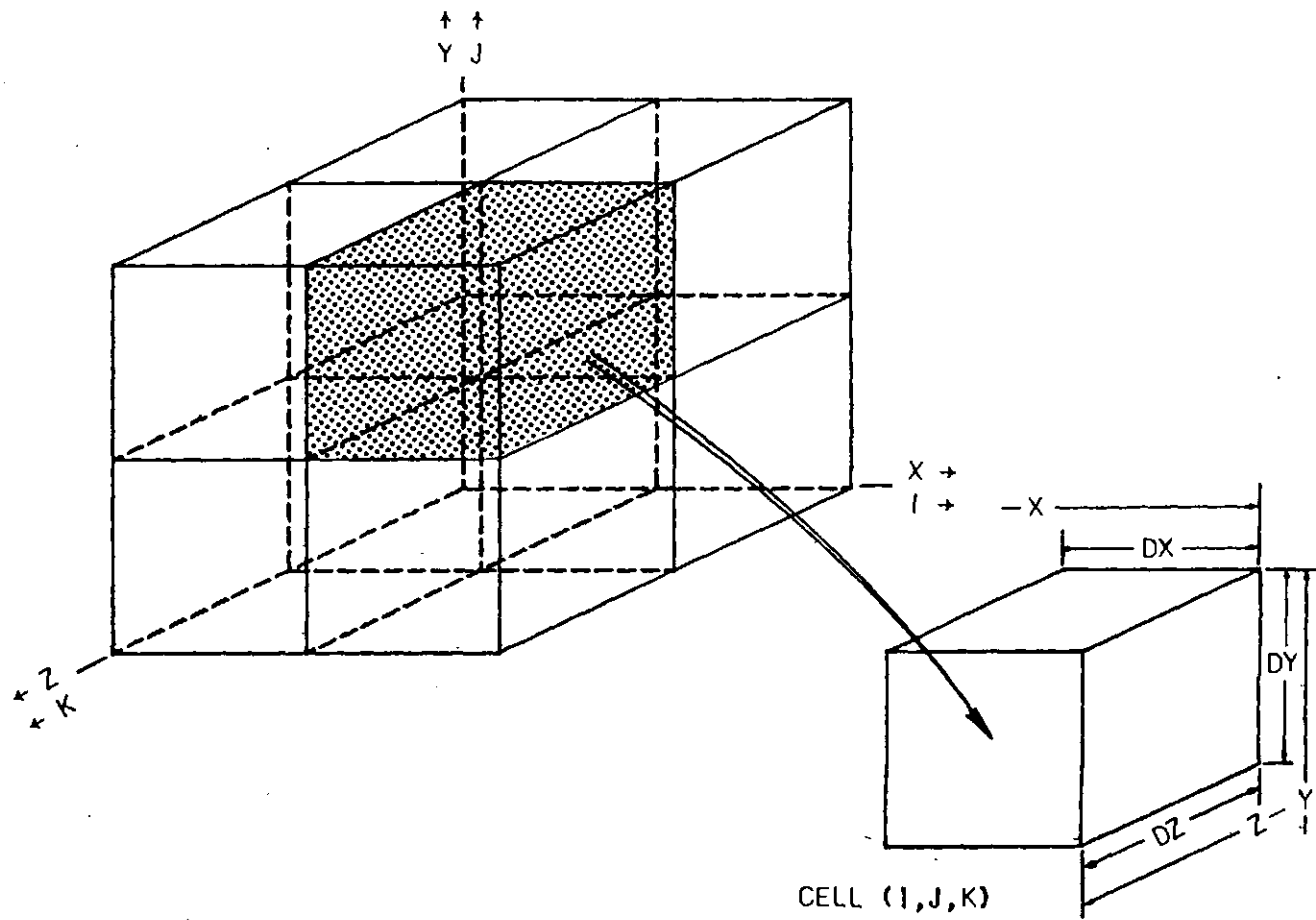


Figure 2. Three-Dimensional Coordinate System

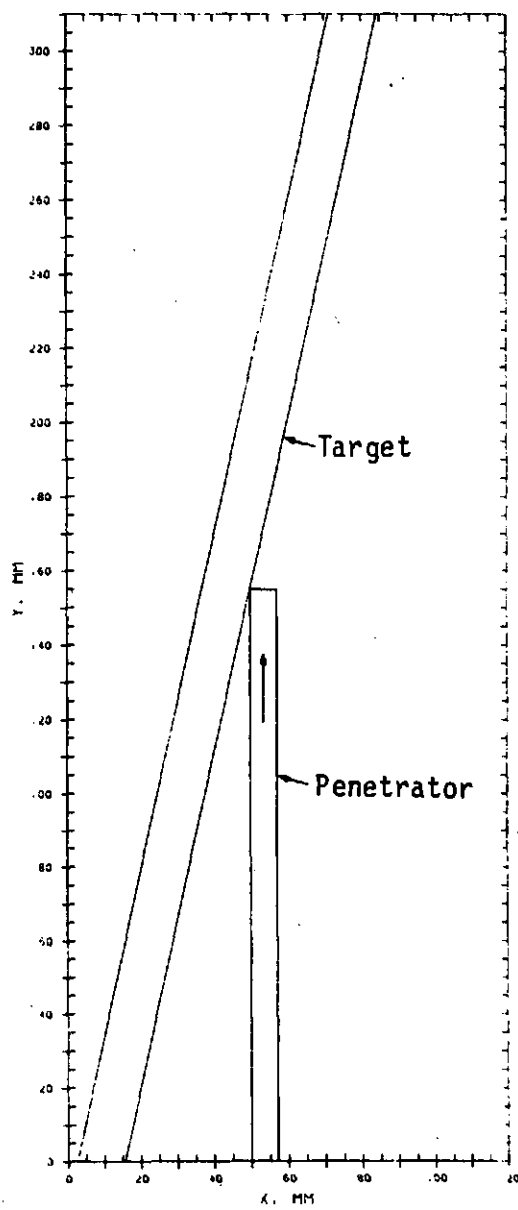


Figure 3. Penetrator-Target Configuration  
in the Plane of Symmetry

77

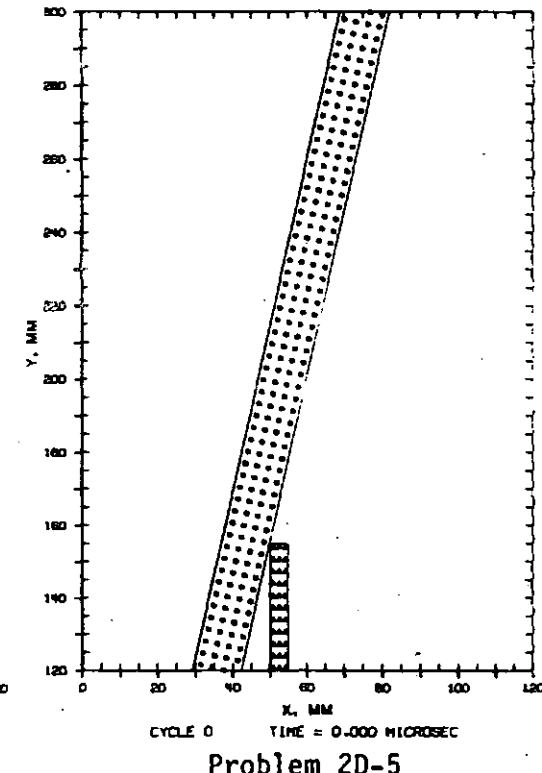
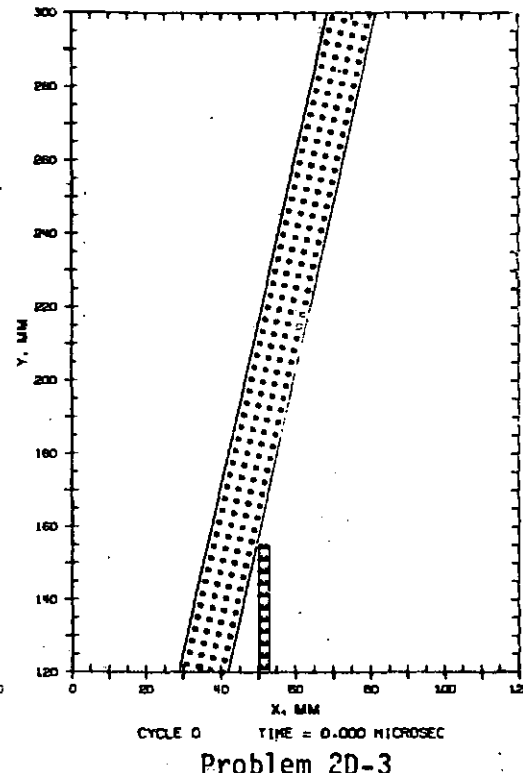
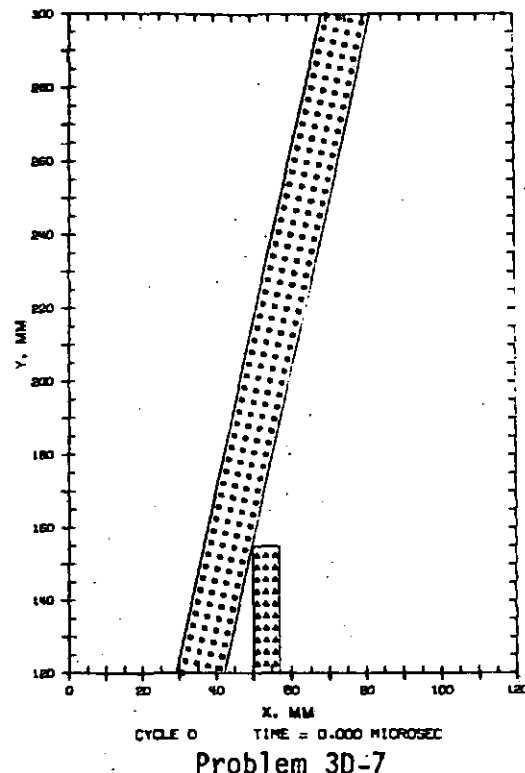
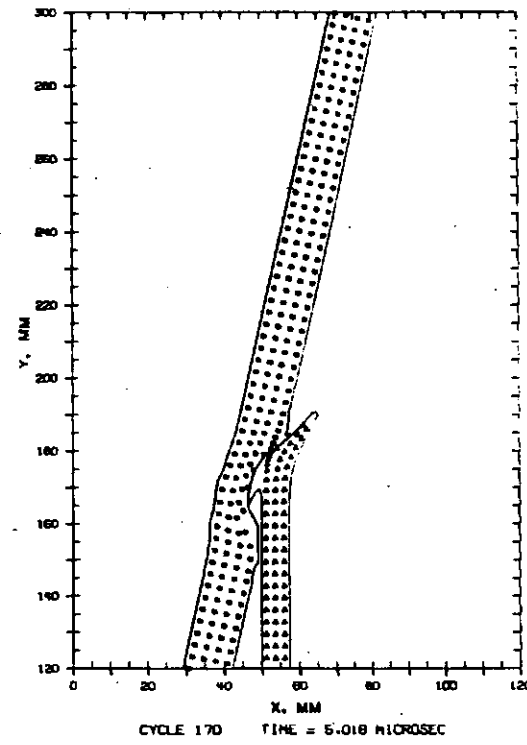
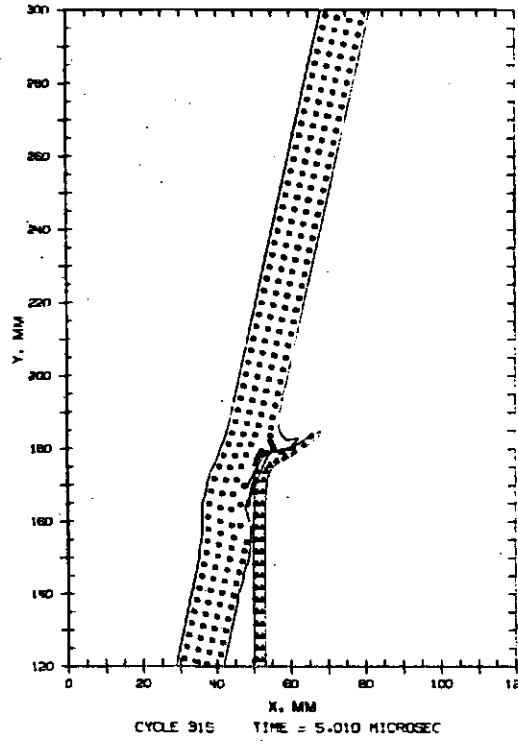


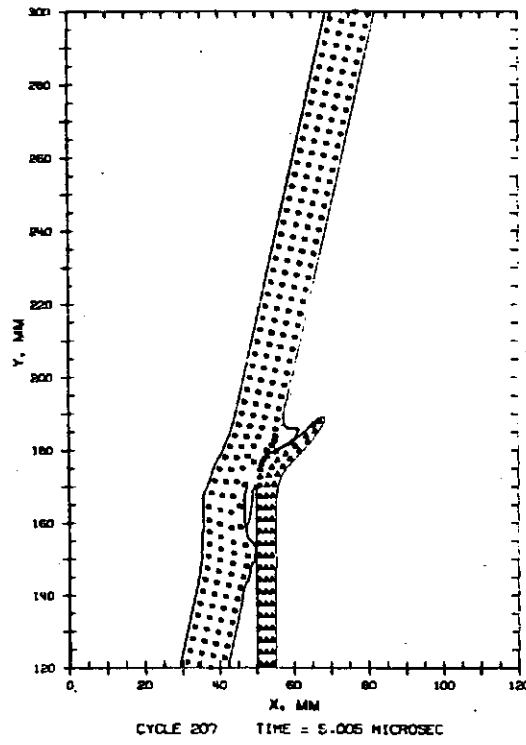
Figure 4. Penetrator-Target Deformations at 0  $\mu$ s.



Problem 3D-7



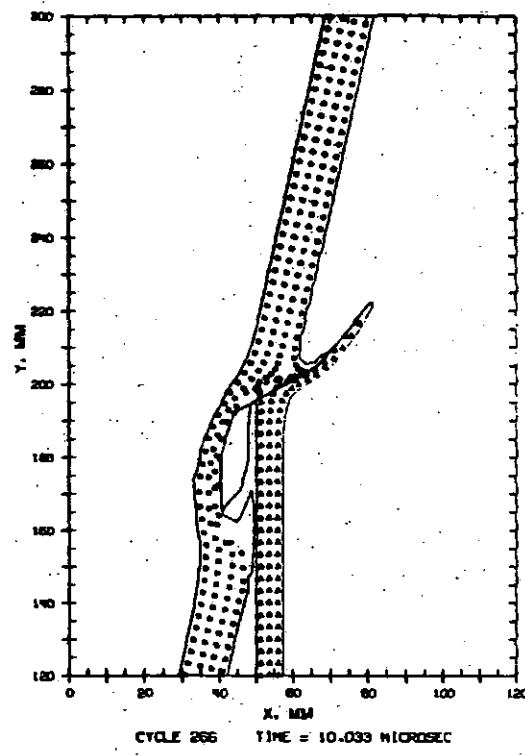
Problem 2D-3



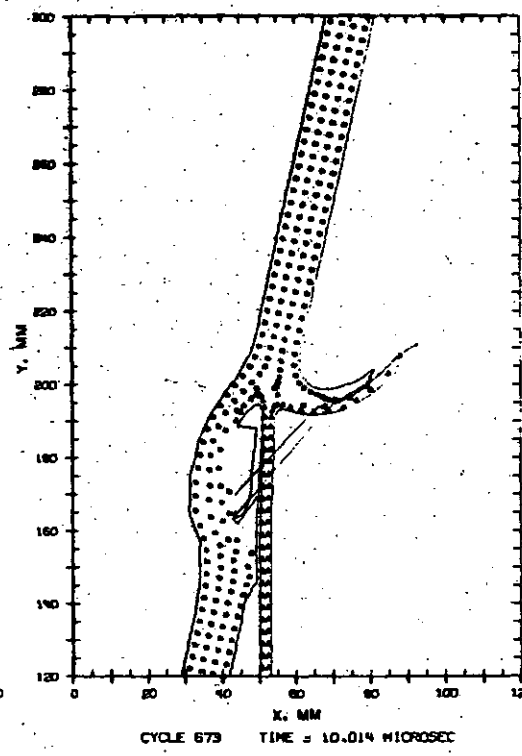
Problem 2D-5

Figure 5. Penetrator-Target Deformations at 5  $\mu$ s.

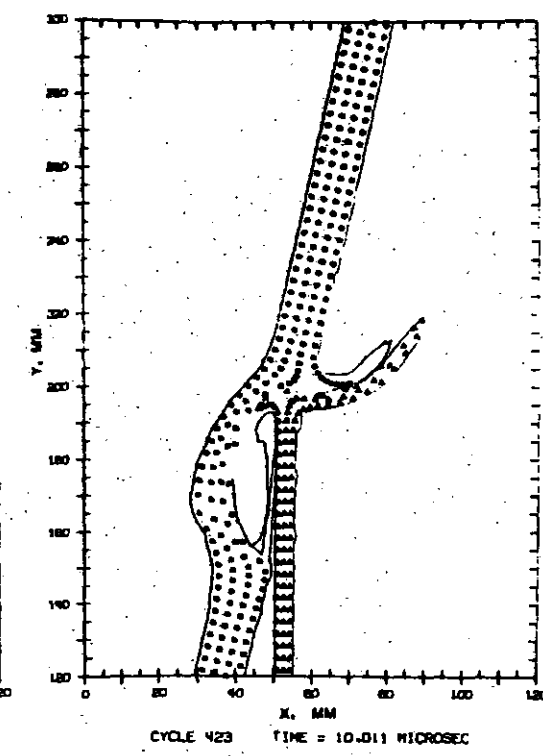
19



Problem 3D-7



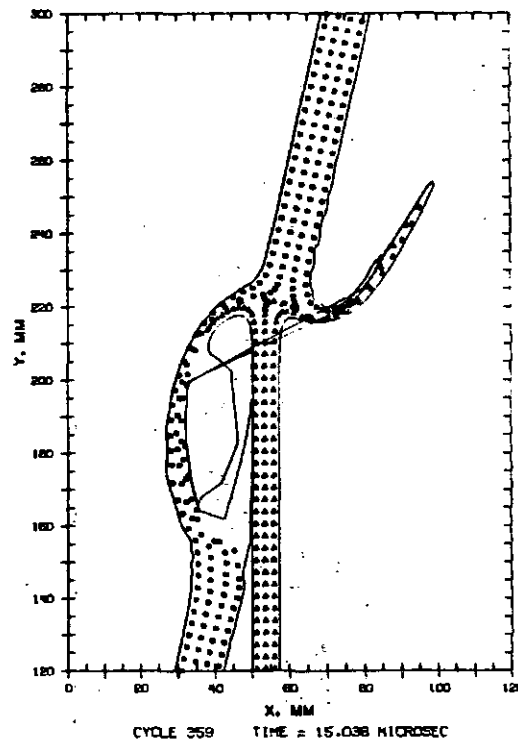
Problem 2D-3



Problem 2D-5

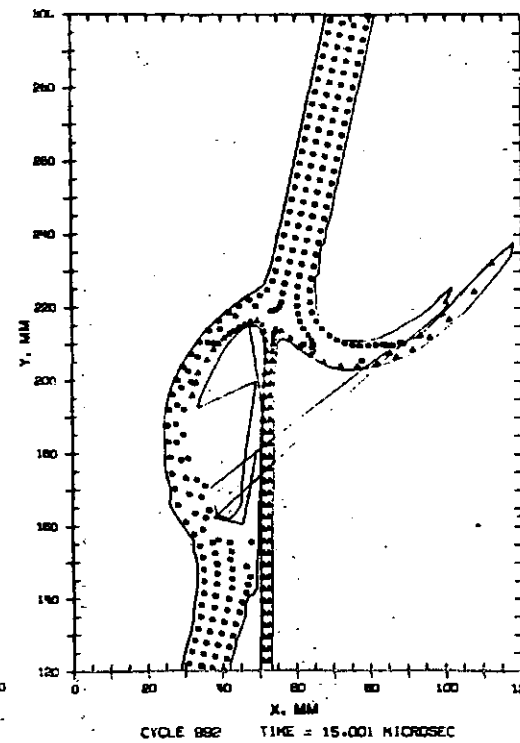
Figure 6. Penetrator-Target Deformations at 10  $\mu$ s.

20



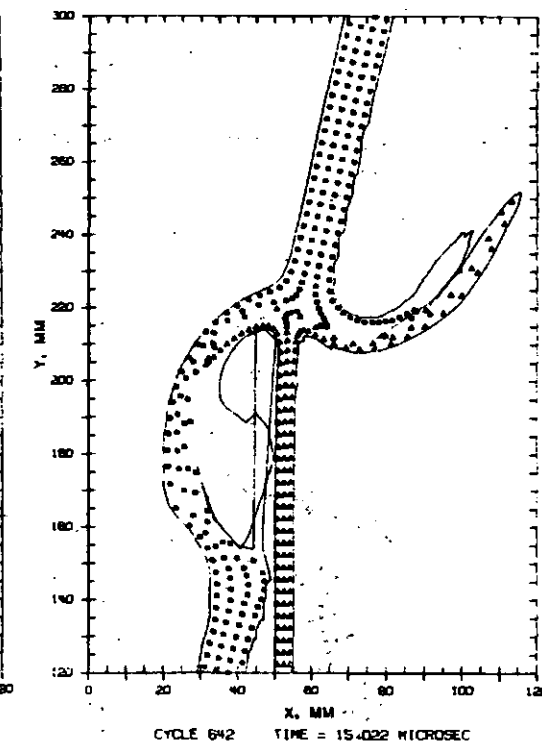
CYCLE 359 TIME = 15.038 MICROSEC

Problem 3D-7



CYCLE 882 TIME = 15.001 MICROSEC

Problem 2D-3

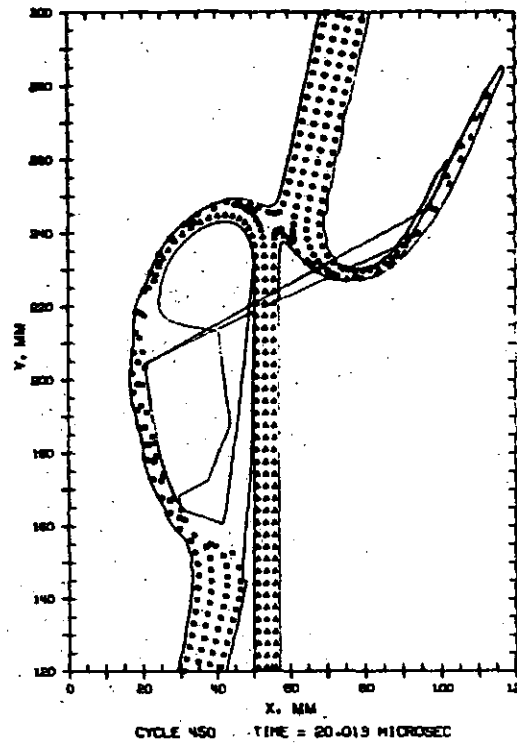


CYCLE 642 TIME = 15.022 MICROSEC

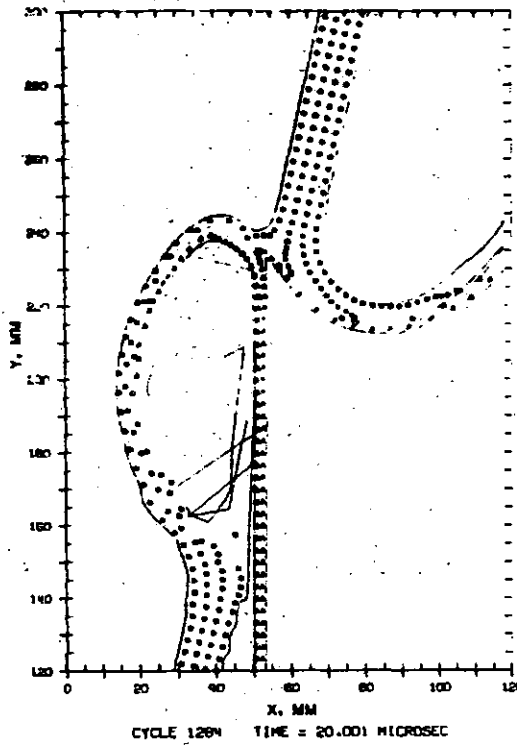
Problem 2D-5

Figure 7. Penetrator-Target Deformations at 15  $\mu$ s.

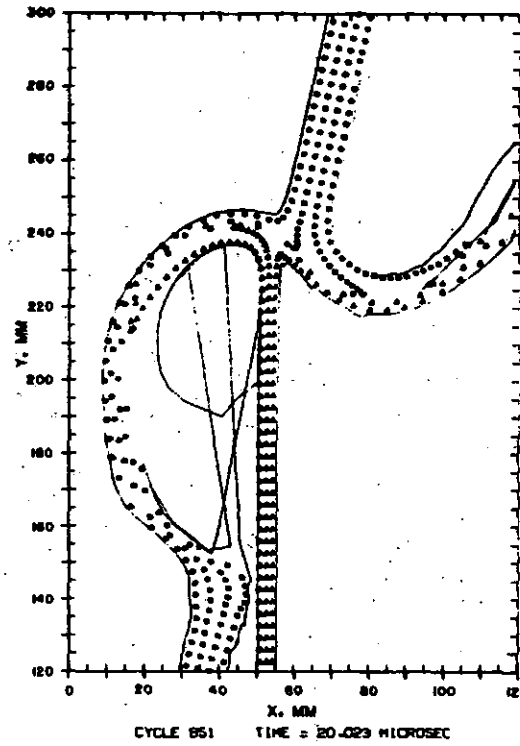
21



Problem 3D-7



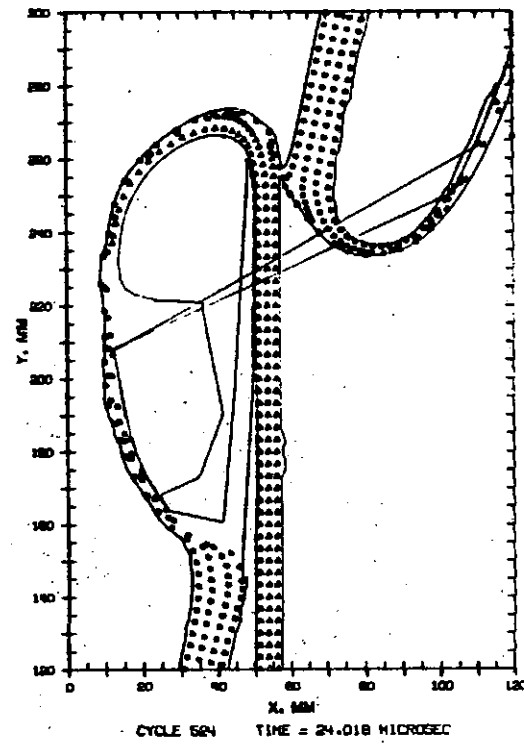
Problem 2D-3



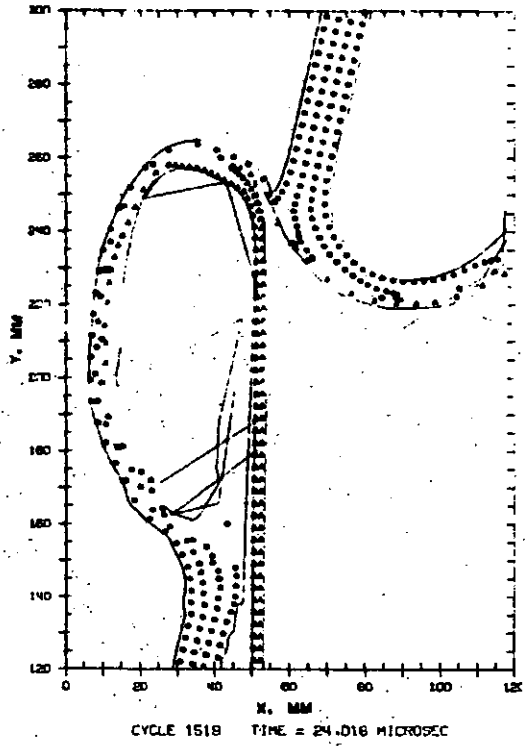
Problem 2D-5

Figure 8. Penetrator-Target Deformations at 20  $\mu$ s.

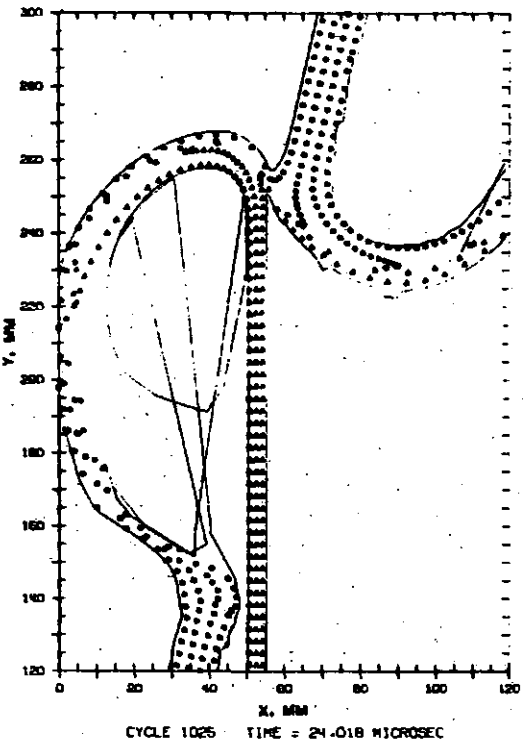
2



Problem 3D-7



Problem 2D-3



Problem 2D-5

Figure 9. Penetrator-Target Deformations at 24  $\mu$ s.

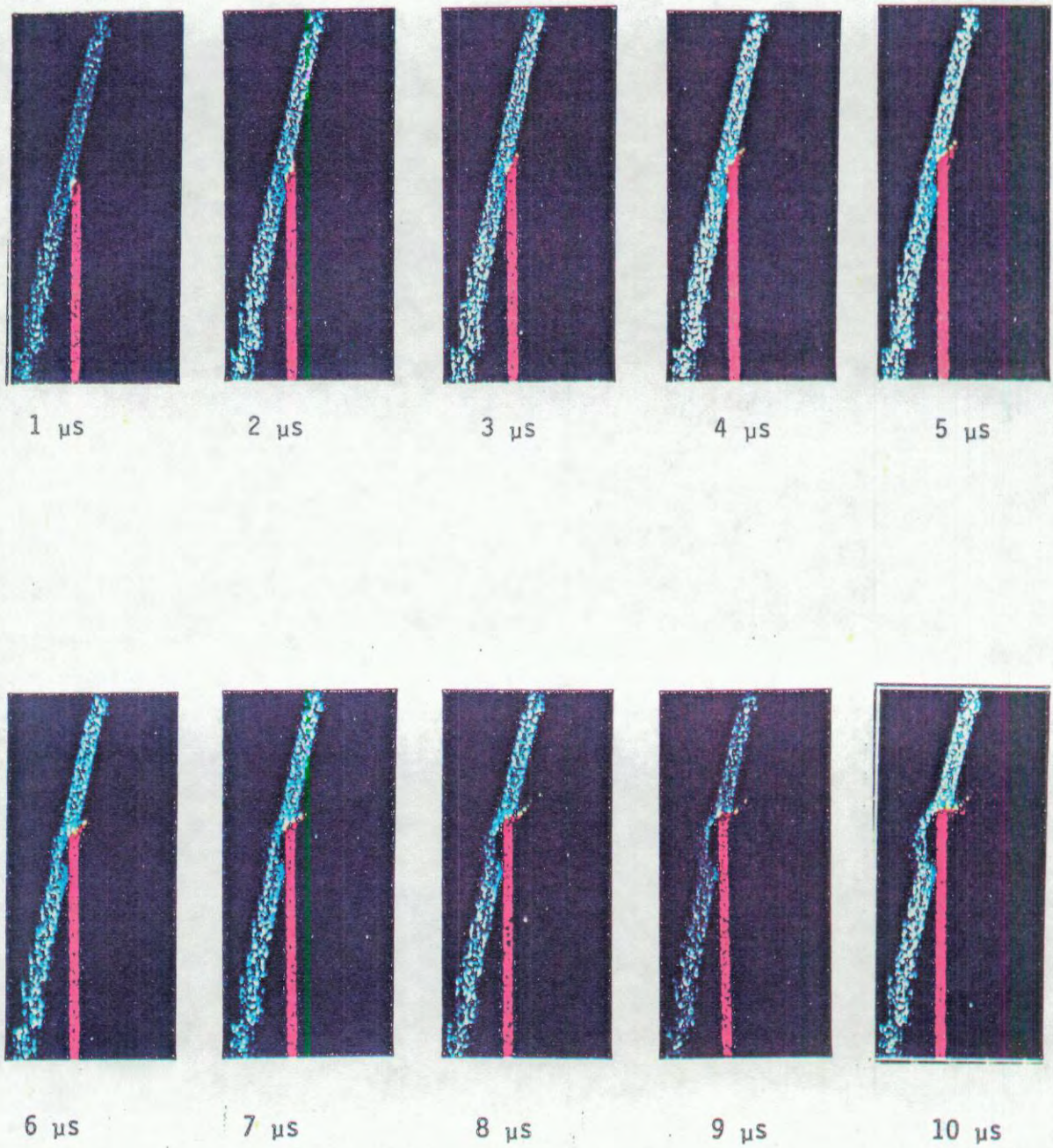


Figure 10. Material Density Plots in the Plane of Symmetry at 1- $\mu$ s Intervals

**This page Left Intentionally Blank**

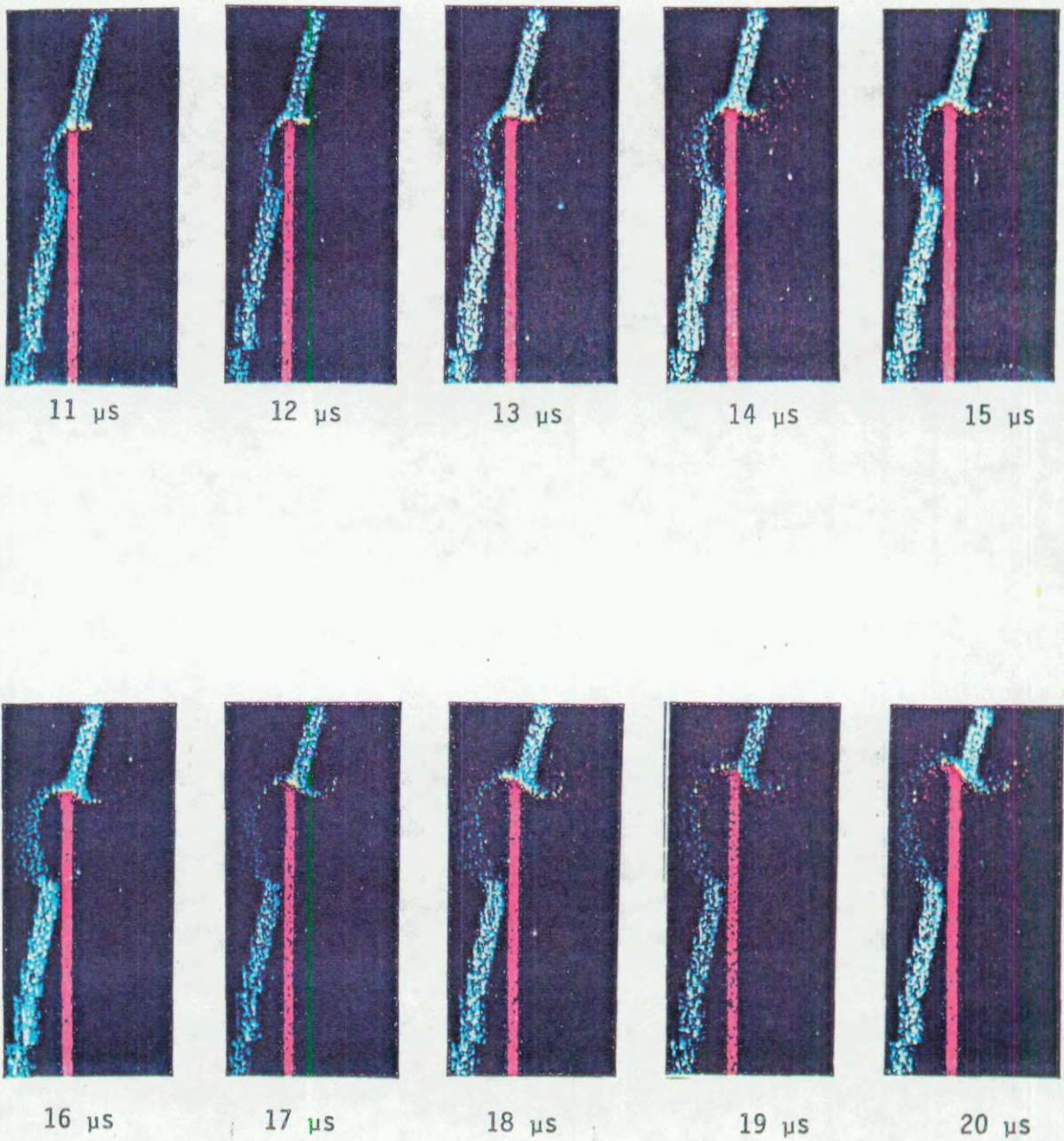


Figure 11. Material Density Plots in the Plane of Symmetry at 1- $\mu$ s Intervals

**This page Left Intentionally Blank**

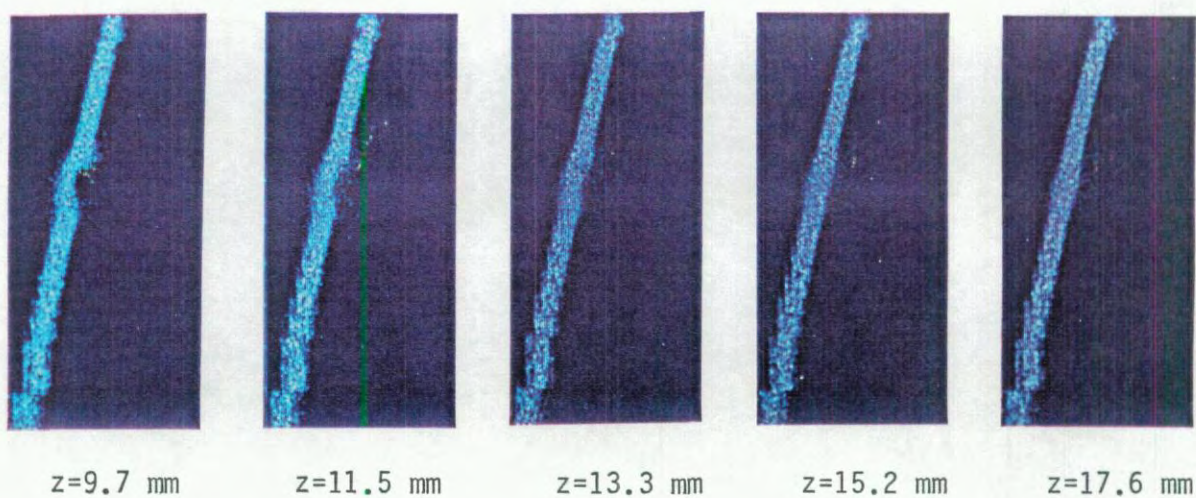
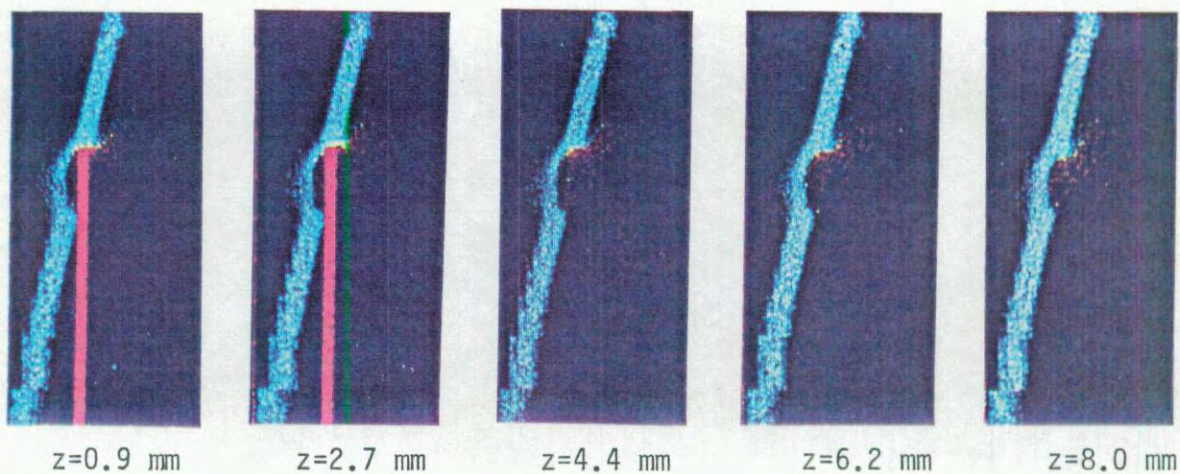


Figure 12. Material Density Plots in Various Z-Planes at  $10 \mu\text{s}$

**This page Left Intentionally Blank**

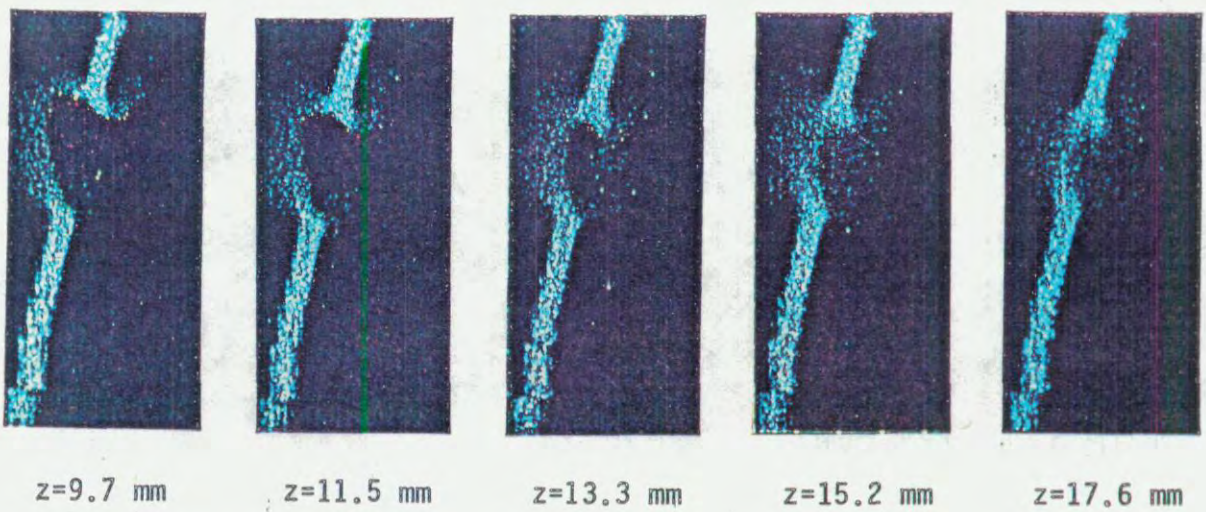
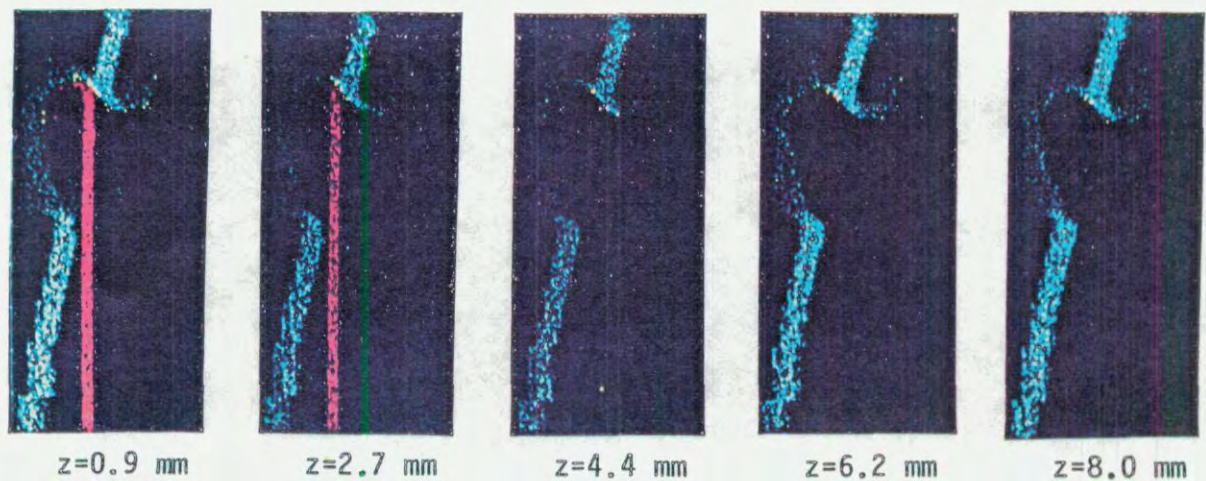


Figure 13. Material Density Plots in Various Z-Planes at 20  $\mu$ s

**This page Left Intentionally Blank**

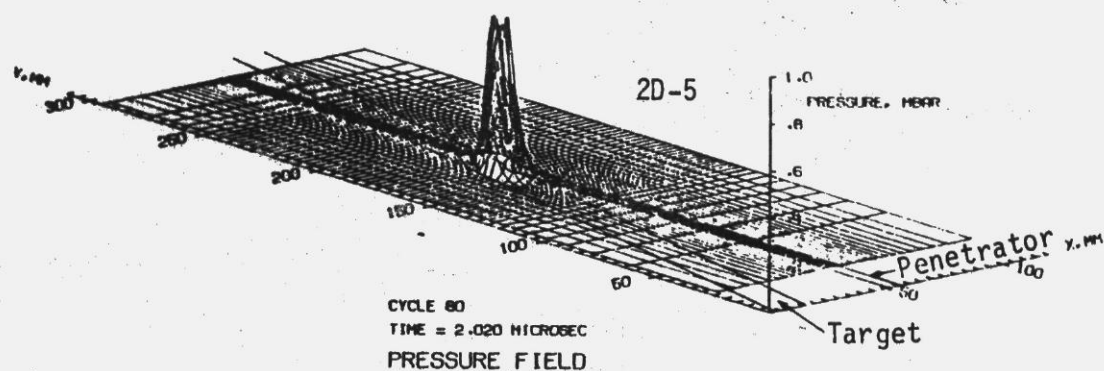
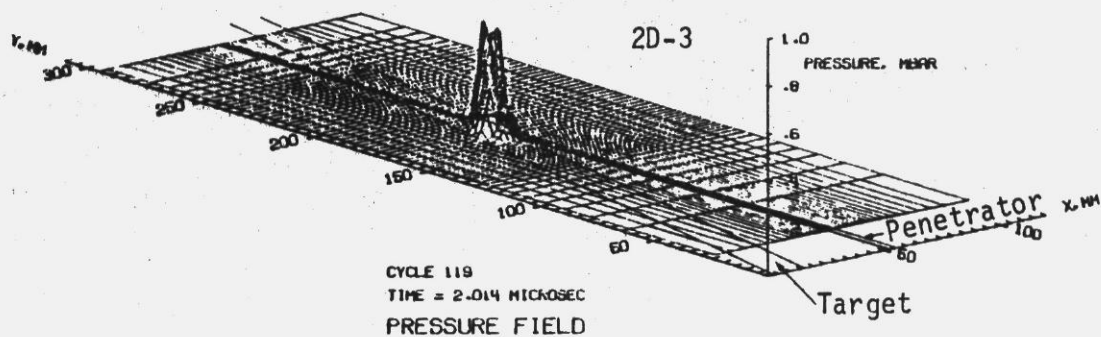
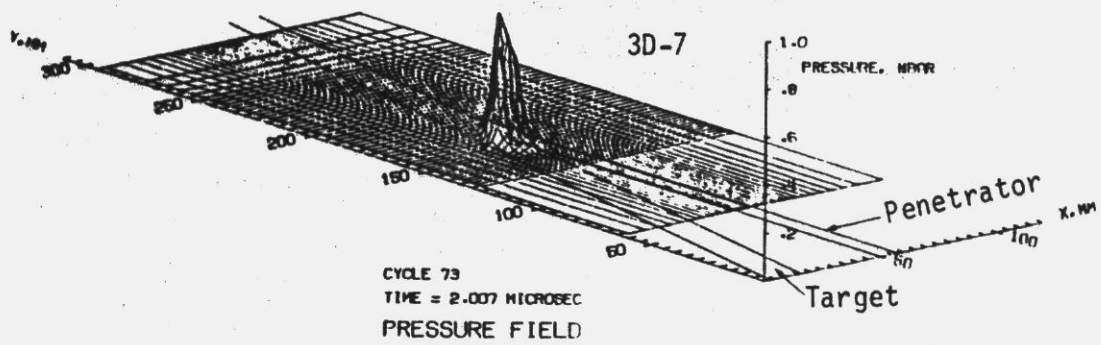


Figure 14. Comparison of Pressure Fields at 2  $\mu$ s

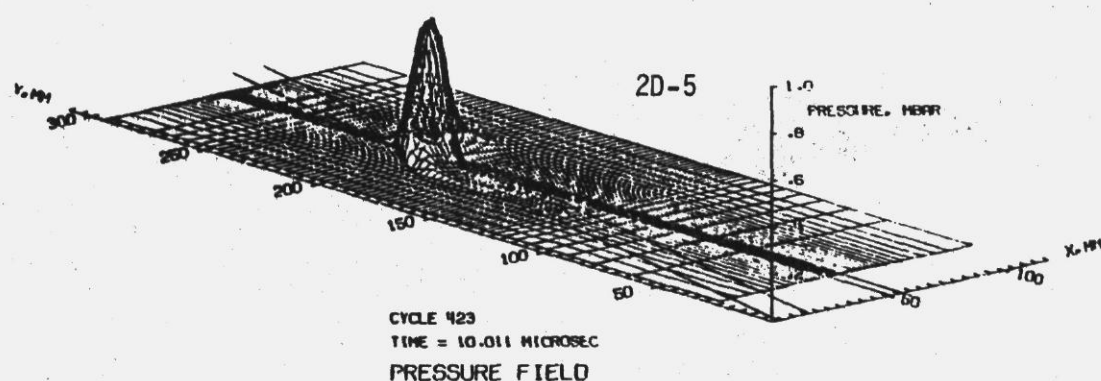
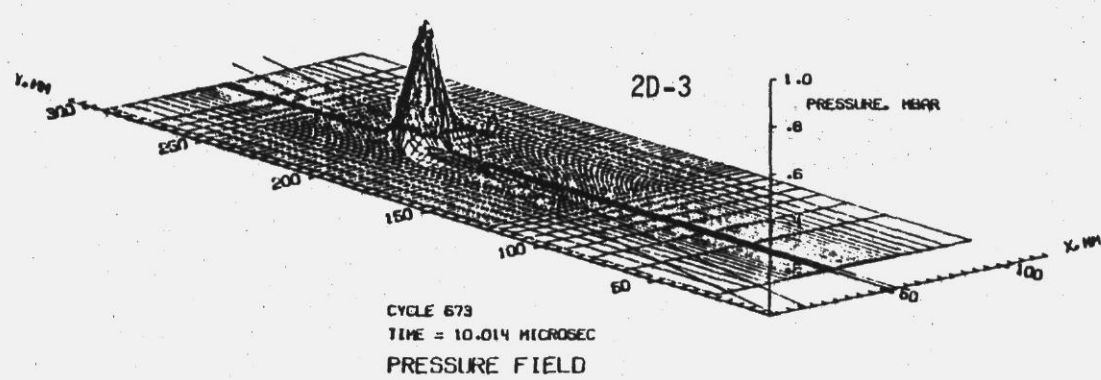
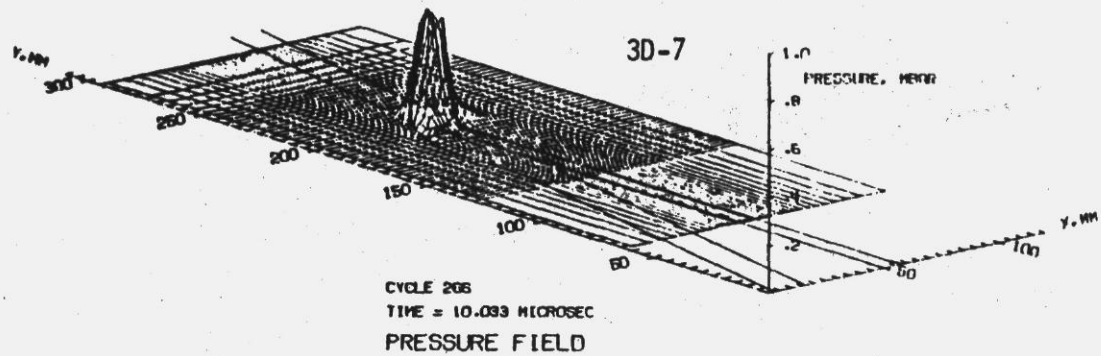


Figure 15. Comparison of Pressure Fields at 10  $\mu$ s

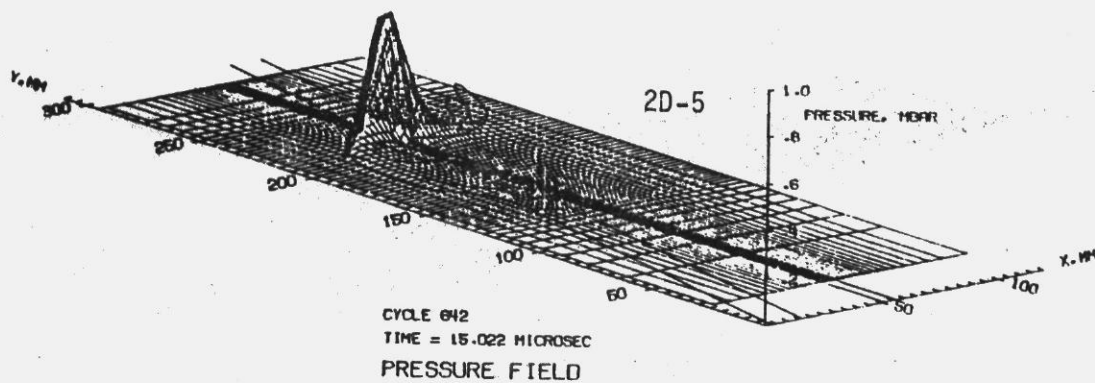
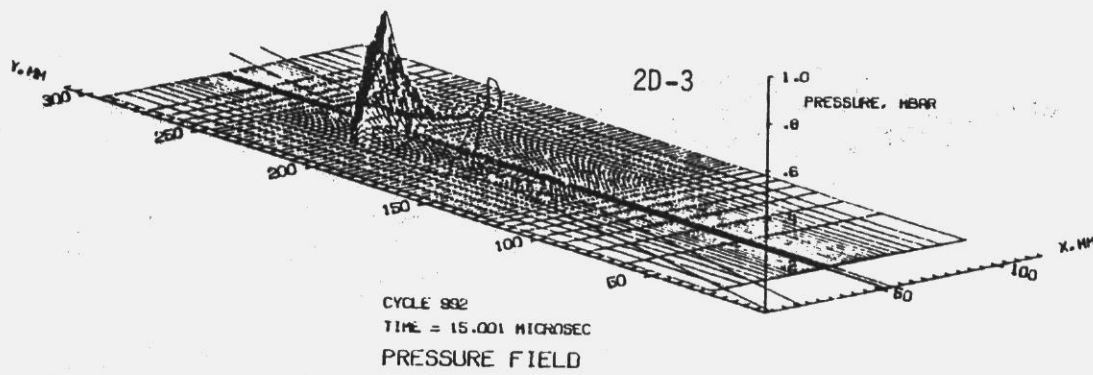
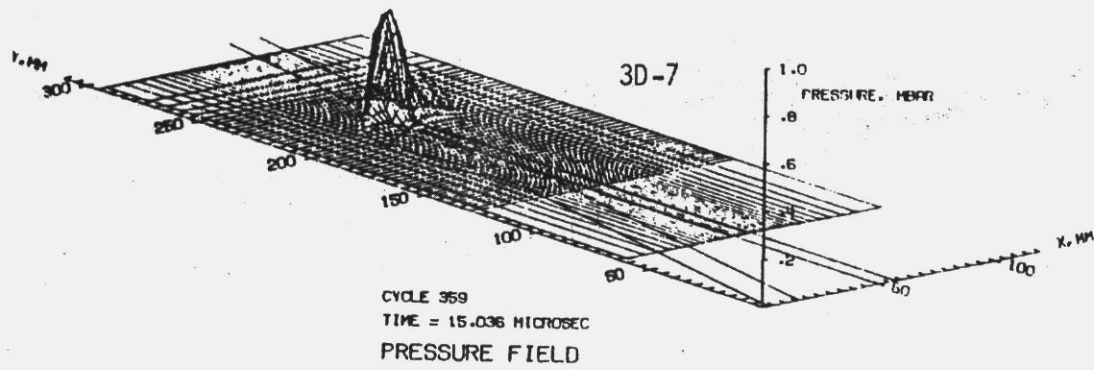


Figure 16. Comparison of Pressure Fields at 15  $\mu$ s

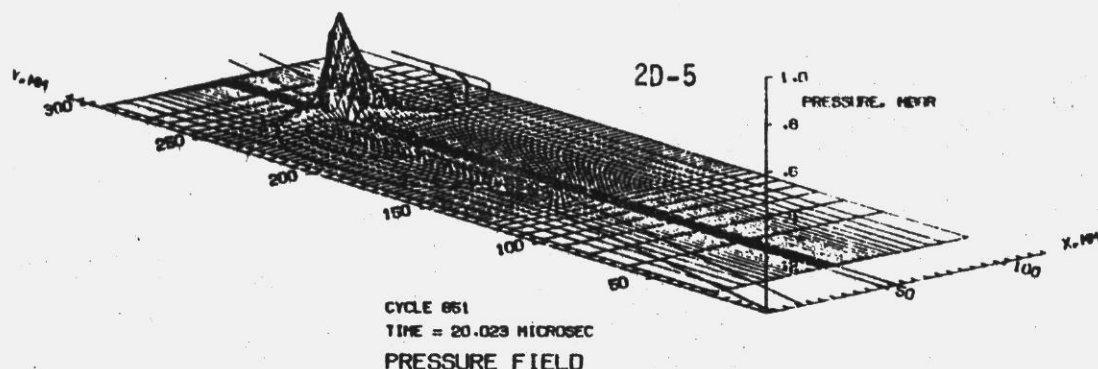
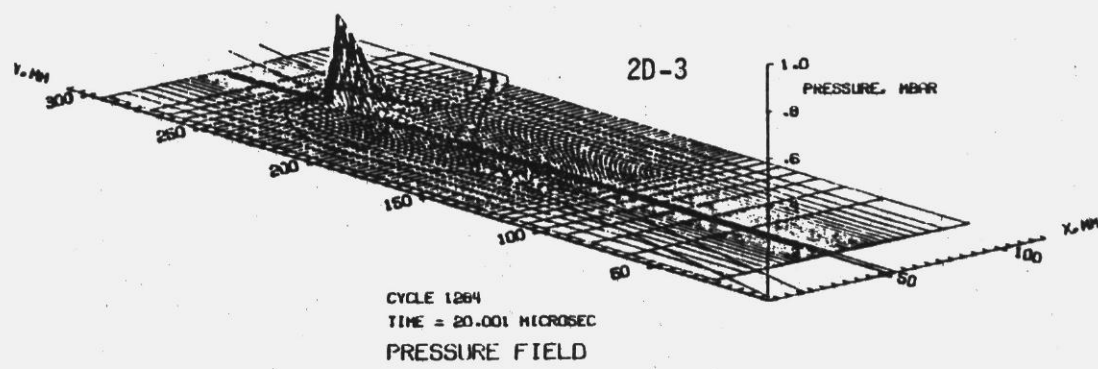
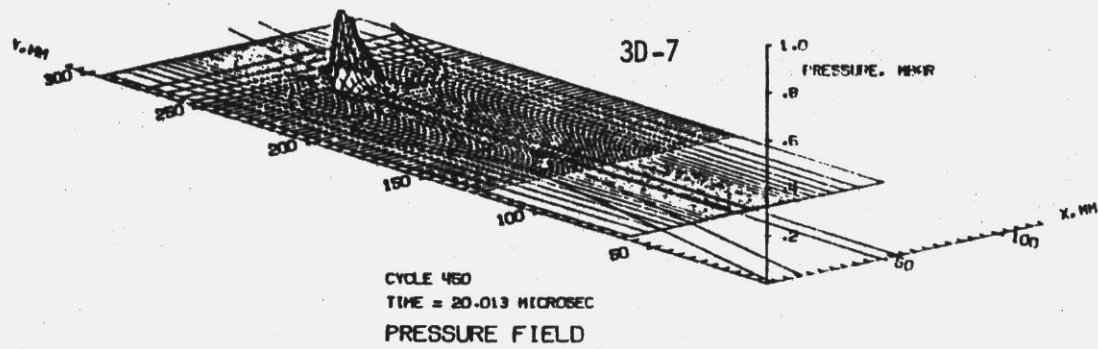


Figure 17. Comparison of Pressure Fields at 20  $\mu$ s

## REFERENCES

1. John T. Harrison, "The History of the Utilization of Eulerian Hydrodynamic Computer Codes at the Ballistic Research Laboratory," Transactions of the Twenty-Fifth Conference of Army Mathematics, ARO Report 80-1, Jun 1979.
2. V. Kucher and J. Harrison, "Shaped-Charge Jet Penetration of Discontinuous Media," Ballistic Research Laboratory Report No. 1995, Jul 1977. (AD #A043845)
3. V. Kucher, "One, Two, and Three-Dimensional Impact Computations," Ballistic Research Laboratory Report ARBRL-TR-02099, Aug 1979. (AD#A060611)
4. W. E. Johnson, "TRIDORF - A Two-Material Version of the TRIOIL Code with Strength," Computer Code Consultants, CCC-976, Sep 1976.
5. J. H. Tillotson, "Metallic Equations of State for Hypervelocity Impact," Gulf General Atomic, GA-3216, Jul 1962.
6. V. Kucher, "Preliminary Computer Computations for Slender Rod Impact Problems," Ballistic Research Laboratory Report No. 1957, Feb 1977. (AD #A036995)

**This page Left Intentionally Blank**

DISTRIBUTION LIST

<u>No. of Copies</u>	<u>Organization</u>	<u>No. of Copies</u>	<u>Organization</u>
12	<p>Commander            Defense Technical Info Center            ATTN: DDC-DDA            Cameron Station            Alexandria, VA 22314</p>	1	<p>Commander            US Army Communications Rsch            and Development Command            ATTN: DRDCO-PPA-SA            Fort Monmouth, NJ 07703</p>
1	<p>Commander            US Army Materiel Development            and Readiness Command            ATTN: DRCDMD-ST            5001 Eisenhower Avenue            Alexandria, VA 22333</p>	1	<p>Commander            US Army Electronics Research            and Development Command            Technical Support Activity            ATTN: DELSD-L            Fort Monmouth, NJ 07703</p>
2	<p>Commander            US Army Armament Research            and Development Command            ATTN: DRDAR-TSS (2 cys)            Dover, NJ 07801</p>	1	<p>Commander            US Army Missile Command            ATTN: DRSMI-R            Redstone Arsenal, AL 35809</p>
1	<p>Commander            US Army Armament Materiel            Readiness Command            ATTN: DRSAR-LEP-L, Tech Lib            Rock Island, IL 61299</p>	1	<p>Commander            US Army Missile Command            ATTN: DRSMI-YDL            Redstone Arsenal, AL 35809</p>
1	<p>Director            US Army ARRADECOM            Benet Weapons Laboratory            ATTN: DRDAR-LCB-TL            Watervliet, NY 12189</p>	1	<p>Commander            US Army Tank Automotive Rsch            and Development Command            ATTN: DRDTA-UL            Warren, MI 48090</p>
1	<p>Commander            US Army Aviation Research            and Development Command            ATTN: DRDAV-E            4300 Goodfellow Blvd            St. Louis, MO 63120</p>	1	<p>Director            US Army TRADOC Systems            Analysis Activity            ATTN: ATAA-SL, Tech Lib            White Sands Missile Range,            NM 88002</p>
1	<p>Director            US Army Air Mobility Research            and Development Laboratory            Ames Research Center            Moffett Field, CA 94035</p>	2	<p>Chief of Naval Research            Department of the Navy            ATTN: Code 427            Code 470            Washington, DC 20360</p>

DISTRIBUTION LIST

<u>No. of Copies</u>	<u>Organization</u>	<u>No. of Copies</u>	<u>Organization</u>
1	Commander US Naval Surface Weapons Center ATTN: Tech Lib Dahlgreen, VA 22448	1	Computer Code Consultants, Inc. ATTN: Mr. W. Johnson 1680 Camino Redondo Los Alamos, NM 87544
1	Commander US Naval Surface Weapons Center ATTN: Code 730, Lib Silver Spring, MD 20910	1	Physics International ATTN: Mr. L. Behrmann 2700 Merced Street San Leandro, CA 94577
1	Commander US Naval Weapons Center ATTN: Code 45, Tech Lib China Lake, CA 93555	1	Sandia Laboratories ATTN: Dr. L. Bertholf Albuquerque, NM 87115
1	Commander US Naval Research Laboratory Washington, DC 20375	1	Systems, Science and Software ATTN: Dr. R. Sedgwick P. O. Box 1620 La Jolla, CA 92037
1	US Air Force Academy ATTN: Code FJS-RL (NC) Tech Lib Colorado Springs, CO 80940	1	Drexel Institute of Technology Wave Propagation Research Center ATTN: Prof. P. Chou 32nd & Chestnut Streets Philadelphia, PA 19104
1	AFWL (SUL) Kirtland AFB, NM 87117	2	University of California Los Alamos Scientific Lab ATTN: Dr. J. M. Walsh Tech Lib P. O. Box 1663 Los Alamos, NM 87545
1	AFLC (MMWMC) Wright-Patterson AFB, OH 45433	1	Shock Hydrodynamics ATTN: Dr. L. Zernow 4710 Vineland Avenue North Hollywood, CA 91602
1	Director National Aeronautics and Space Administration Langley Research Center Langley Station Hampton, VA 23365	1	Southwest Research Institute Dept of Mechanical Sciences ATTN: Mr. A. Wenzel 8500 Culebra Road San Antonio, TX 78228
4	Director Lawrence Livermore Laboratory ATTN: Mr. M. Wilkins Dr. C. Godfrey Dr. G. Goudreau Dr. R. Werne P. O. Box 808 Livermore, CA 94550		

DISTRIBUTION LIST

<u>No. of</u>	<u>Copies</u>	<u>Organization</u>	<u>No. of</u>	<u>Copies</u>	<u>Organization</u>
3		Honeywell, Inc. Government and Aerospace Products Division ATTN: Mr. J. Blackburn Dr. G. Johnson Mr. R. Simpson 600 Second Street, NE Hopkins, MN 55343			Aberdeen Proving Ground Dir, USAMSAA ATTN: DRXSY-D* DRXSY-MP, H. Cohen Cdr, USATECOM ATTN: DRSTE-TO-F DIR, USACSL Bldg. E3516, EA ATTN: DRDAR-CLB-PA

### USER EVALUATION OF REPORT

Please take a few minutes to answer the questions below; tear out this sheet, fold as indicated, staple or tape closed, and place in the mail. Your comments will provide us with information for improving future reports.

1. BRL Report Number \_\_\_\_\_
2. Does this report satisfy a need? (Comment on purpose, related project, or other area of interest for which report will be used.)  
\_\_\_\_\_  
\_\_\_\_\_  
\_\_\_\_\_
3. How, specifically, is the report being used? (Information source, design data or procedure, management procedure, source of ideas, etc.)  
\_\_\_\_\_  
\_\_\_\_\_  
\_\_\_\_\_
4. Has the information in this report led to any quantitative savings as far as man-hours/contract dollars saved, operating costs avoided, efficiencies achieved, etc.? If so, please elaborate.  
\_\_\_\_\_  
\_\_\_\_\_  
\_\_\_\_\_
5. General Comments (Indicate what you think should be changed to make this report and future reports of this type more responsive to your needs, more usable, improve readability, etc.)  
\_\_\_\_\_  
\_\_\_\_\_  
\_\_\_\_\_
6. If you would like to be contacted by the personnel who prepared this report to raise specific questions or discuss the topic, please fill in the following information.

Name: \_\_\_\_\_

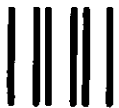
Telephone Number: \_\_\_\_\_

Organization Address: \_\_\_\_\_

\_\_\_\_\_  
\_\_\_\_\_

— FOLD HERE —

Director  
US Army Ballistic Research Laboratory  
Aberdeen Proving Ground, MD 21005



NO POSTAGE  
NECESSARY  
IF MAILED  
IN THE  
UNITED STATES

OFFICIAL BUSINESS  
PENALTY FOR PRIVATE USE, \$300

**BUSINESS REPLY MAIL**  
FIRST CLASS PERMIT NO 12062 WASHINGTON, DC  
POSTAGE WILL BE PAID BY DEPARTMENT OF THE ARMY

Director  
US Army Ballistic Research Laboratory  
ATTN: DRDAR-TSB  
Aberdeen Proving Ground, MD 21005



— FOLD HERE —